Design and Field Tests of a Directly Coupled Waveguide-On-Access-Tube Soil Water Sensor

J. J. Casanova, R. C. Schwartz, S. R. Evett

Abstract. *Sensor systems capable of monitoring soil water content can provide a useful tool for irrigation control. Current systems are limited by installation depth and labor, accuracy, and cost. Time domain reflectometry (TDR) is an approach for monitoring soil water content that relates the travel time of an electromagnetic pulse on a waveguide to the water content of the soil. This article discusses the design, installation, lab testing, and field testing of a novel TDR sensor, using a multi-segmented, waveguide-on-access-tube (WOAT) geometry. The segmented WOAT approach allows for ease of assembly and installation of the sensor stack to the desired depth. Additionally, this sensor incorporates circuits embedded in the sensor body itself, directly coupled to the waveguides, eliminating problems associated with cabling encountered in previous WOAT embodiments. Despite some initial problems with mechanical strength of the prototype sensors, the WOAT equipment provided quality TDR waveforms and long-time reflection coefficients on a daily basis at multiple depths over the course of several months, providing data for both soil water content and bulk electrical conductivity estimates. When properly calibrated, the WOAT data were comparable to concurrent measurements of soil water content using a neutron probe, though there were differences due to the disparity in sensing volumes. Overall, we show that this is a promising new sensor design.*

Keywords. *Sensors, Soil water, Digital, TDR, Electromagnetics.*

Soil water content is an important metric for managing timing and amounts of irrigation (Merriam, 1966; Evett et al., 2009). Due to the large rooting depth of some crops, measurements of the soil water profile greater than 2 m are necessary in some cases to accurately capture the root zone soil water dynamics, particularly for soil water balance studies of crop water use (Evett et al., 2012). Time-domain reflectometry (TDR) uses the travel time (t_t) of an electric pulse sent down a waveguide of length L surrounded by the medium to be measured (Topp et al., 1980). The travel time is related to the apparent soil permittivity, ε_a, by the relationship $\varepsilon_a = (c_0\, t_t /2L)^2$, where c_0 is the speed of light in a vacuum. Although travel time is predominantly a function of soil water content, it can also be affected by pulse bandwidth, soil bulk electrical conductivity (σ_a), bound water content, and temperature (Schwartz, 2009a).

This article considers a TDR geometry consisting of a cylindrical access tube segment with surface-mounted electrodes. The system is a waveguide-on-access-tube (WOAT) and a cross section is shown in figure 1. This particular WOAT system is unique because it incorporates miniaturized TDR circuitry in each WOAT segment, one circuit for each of the two waveguides on each segment. Evett et al. (2009) demonstrated that commercially available down-hole EM sensors that rely on a fringing field to estimate water content were rendered inaccurate and imprecise by small scale (less than 1 cm) variations in electromagnetic (EM) soil properties. Using a time domain measurement, the WOAT technology is inherently more accurate and precise, despite small-scale variations in soil structure and bulk electric conductivity (BEC) (Evett et al., 2012). This design permits the installation of sensors to depths of greater than 2 m, which are not easily attained using conventional TDR probes without significant soil disturbance. Previous work on this design investigated the electromagnetic theory of the WOAT design and tested laboratory prototypes to determine the effects of variations in geometry and the properties of the soil (Casanova et al., 2012a; Casanova et al., 2012b). Field tests of a 1.6-m WOAT sensor comprised of eight 20-cm segments (Casanova et al., 2012c) demonstrated the practical feasibility of the WOAT design, but utilized mechanical connections of the electrodes of each waveguide to separate coaxial cables in the interior of the access tube. The coaxial cables passed through the length of the access tube to a coaxial multiplexer (Evett, 1998) outside the access tube and through the multiplexer to a TDR instrument (model 1502C, Tektronix, Redmond, Oreg.).

Submitted for review in April 2013 as manuscript number IET 10207; approved for publication by the Information & Electrical Technologies Division of ASABE in September 2013.

The use of trade, firm, or corporation names in this article is for the information and convenience of the reader. Such use does not constitute an official endorsement or approval by the United States Department of Agriculture or the Agricultural Research Service of any product or service to the exclusion of others that may be suitable.

The authors are **Joaquin J. Casanova, ASABE Member,** Research Agricultural Engineer, **Steven R. Evett, ASABE Member,** Research Soil Scientist, and **Robert C. Schwartz, Research Soil Scientist,** USDA-ARS Conservation and Production Research Laboratory, Bushland, Texas. **Corresponding author:** Joaquin J. Casanova, USDA-ARS Conservation and Production Research Laboratory, P.O. Drawer 10, Bushland, TX 79012; phone: 806-356-5718; email: joaquin.casanova@gmail.com.

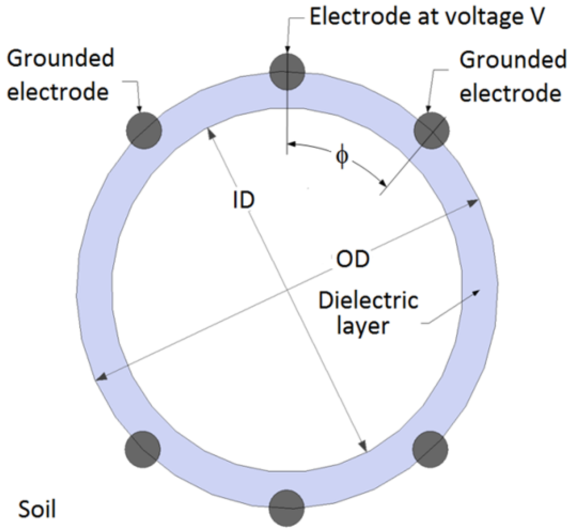

Figure 1. Cross-section of access-tube design. OD is outside diameter, 73.03 mm; ID is inside diameter, 57.15 mm; ϕ is electrode spacing angle, 45°.

The TDR instrument was controlled and interrogated by a computer running the TACQ program (Evett, 2000a,b), which also controlled the multiplexer to acquire waveforms and long-time reflection coefficients from each waveguide. The mechanical connections and long coaxial cables led to an unacceptable amount of measurement uncertainty in travel time due to noise and waveform variability, as well as being difficult to connect and prone to disconnection during the field experiment.

Here, we present the design details, lab calibration, field installation, and field data acquisition of a WOAT sensor for soil water content and BEC determination. This new design addresses the problems found in the previous field experiment by using a modular, segmented design, with TDR circuits embedded in the wall of each WOAT segment, eliminating the coaxial cables, the multiplexer, and the connections between these and the waveguides. In the previous design, the unreliable mechanical connections resulted in connections being lost entirely. Those problems are eliminated with the new design. Since the two designs were not tested concurrently, a direct comparison is not possible; however, a thorough laboratory comparison of the directly-coupled digital and conventional analog WOATs is presented in Casanova et al. (2013). Objectives of the study were to field install multi-segment stacks of the new sensors, study and report on any difficulties in installation, and acquire water content and BEC data in the field for comparison with data from the neutron probe and from previously published values of BEC for the soil studied.

MATERIALS AND METHODS

DESIGN AND INSTALLATION PROCEDURE

The WOAT design is fundamentally a cylindrical tube with electrodes on the exterior serving as waveguides. A cross section of the design can be seen in figure 1. Initial prototypes were constructed of 73 mm outside diameter, schedule 40 rigid polyvinyl chloride (PVC) and tested with Acclima TDR circuits (Meridian, Idaho) directly coupled to the electrodes (Casanova et al., 2013). After tests proved successful, a design with similar geometry but with a slot in the tube wall for the circuit was drafted using a computer-aided design (CAD) program (Trimble SketchUp, Sunnyvale, Calif.). This design was fabricated using stereolithography (SLA) to test for form and fit, shown in figure 2, by a rapid prototyping company (Quickparts, Atlanta, Ga.). Finally, the design was refined and a run of sensor bodies was manufactured by casting plastic similar to acrylonitrile butadiene styrene (ABS) in a urethane mold. ABS has a relative dielectric constant of 2.4 at 60 MHz (Redeye, 2008). The design (fig. 3) incorporated several key features. The TDR circuit was placed in the tube wall in a properly sized slot. Additionally, communications and power connected to a central bus that allowed the

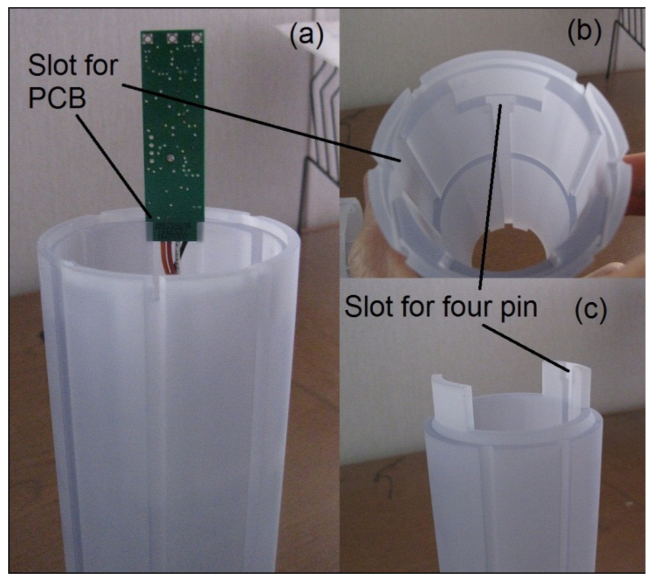

Figure 2. Stereolithograhy (SLA) prototype showing slots for time domain reflectometry printed circuit board (PCB) and for buss and four-pin connectors: (a) side view; (b) bottom view; (c) top view.

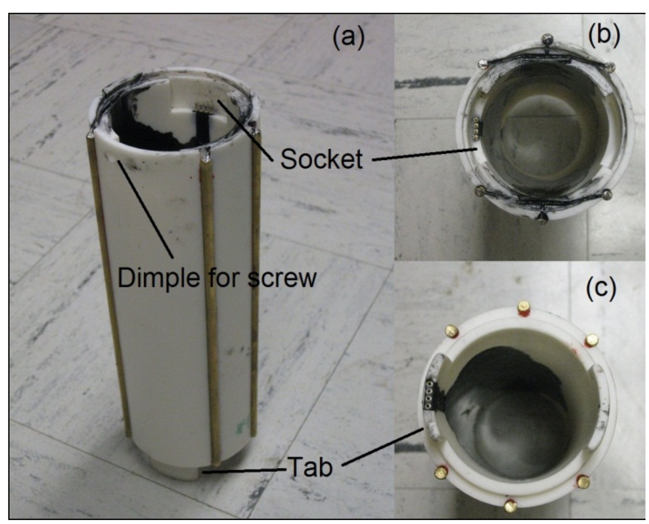

Figure 3. Fully assembled WOAT segment after potting of circuits with black epoxy resin potting compound: (a) side view; (b) bottom view; (c) top view.

sensor segments to link together by four-pin connectors. To keep the segments together, there were mating prongs on one end of each segment and mating slots on the opposite end. A small groove allowed for an O-ring to seal the connection.

Individual segments were assembled as follows. First, naval bronze electrodes (4.8 mm diameter, 195 mm long) were connected to the circuits with 22 gauge buss wire. The electrodes were seated in the grooves with room-temperature vulcanizing (RTV) silicone. The circuits buss cable, and four-pin connectors were glued in place using RTV silicone; and after the silicone cured, the interior recesses containing circuitry were filled with epoxy potting compound to seal the circuits from moisture. The segments were linked together as needed prior to or during installation by placing an O-ring and a thin bead of RTV silicone, followed by fastening segments together with machine screws that passed through the plastic body and into the tab of the adjacent segment.

Installation proceeded using a method similar to that described in Casanova (2012c), using a hydraulic press to incrementally push the assembled WOAT stack with a leading cutting edge into the soil after hand-augering soil slightly ahead of the cutting edge from the interior of the WOAT. Initial installation attempts used a fully assembled WOAT stack (fig. 4a) with a beveled cutting edge affixed to the bottom edge (fig. 4b). A removable steel tube on the interior transferred force from the hydraulic push press to the cutting edge, and a steel cap transferred the force from the hydraulic press to both the WOAT stack and the steel tube. Pieces of rigid PVC tubing were machined to fit into opposite ends of the WOAT segment stack in order to mate the cutting edge and top cap to the stack such that, initially, push force was transferred to both the plastic WOAT stack and the steel tube equally. Later attempts used a guiding tripod (fig. 4c) and assembled the stack as it was pushed into the ground, using steel tubes cut to different lengths to transfer force as the installation proceeded.

Lab Tests

One 20-cm WOAT segment was constructed and used to determine a calibration curve and probe constant. Since the probe measures a dielectric that is a mix of the soil, plastic tube body, and air within the tube, we opted to determine a calibration curve relating the measured volumetric soil water content (VSW) to the measured travel time (t_t). This curve was established by means of creating mixtures of soil (Pullman Ap silty clay loam) at particular levels of VSW, from air dry to fully saturated, following the methods of Casanova et al. (2012b), and acquiring TDR waveforms in each. Soil was mixed in sealed containers on a rotating mixer with water to achieve a desired water content (from dry to 0.20 m^3/m^3, in increments of nominally 0.05 m^3/m^3); then packed around the sensor in a 0.203-m diameter, 0.216-m high PVC cylinder, (sufficient to contain one 20-cm WOAT segment) to the desired bulk density (1.27 Mg/m^3, the highest consistently achievable in the laboratory) and the sensor-soil-container system was weighed. Waveforms were acquired, and then gravimetric samples were taken to assess actual water content. Sensor evaluation at or near saturation was achieved by introducing deionized water at the bottom of the packed column at a small positive pressure head while cylinder mass was determined using a load cell. A single column was prepared at each water content for the evaluation of the sensor response, beginning with dry soil. Values between 0.2 m^3/m^3 and saturation were not tested due to the difficulty of achieving a homogeneous soil sample at these water contents.

Additionally, a probe constant related the long-time reflection coefficient of the TDR waveform to the BEC of the medium, using the method of Lin et al. (2008). The probe constant was determined by waveform acquisition in KCl solutions of known conductivity, and with long-time reflection coefficients scaled using open and short circuit conditions.

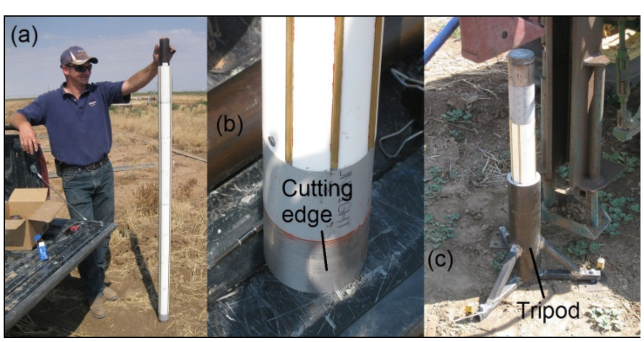

Figure 4. Installation: (a) assembled WOAT stack; (b) cutting edge; (c) guide tripod that was used for later installations in the wet site.

Field Tests

The test location included a dry site to which no irrigations were applied and a wet site that was periodically flood irrigated to wet the profile. Due to the drought conditions, the dry site was extremely dry (0.23 m^3/m^3). The field experiments were conducted at the USDA-ARS, Conservation and Production Research Laboratory (CPRL) at Bushland, Texas (35° 11’ N, 102° 06’ W, 1170 m elev. above MSL) in a Pullman fine, mixed, superactive, thermic Torrertic Paleustoll. The soil profile consisted of an A horizon from 0 to 20 cm depth containing about 35% clay, a Bt horizon extending from 20 to 110 cm depth containing up to 50% clay, and Btk horizon below 110 cm depth containing ~50% $CaCO_3$ in a clayey caliche matrix. Bulk density varies with depth, being ~1.35 Mg/m^3 in the A horizon, increasing to 1.55 Mg/m^3 in the Bt horizon and decreasing to ~1.42 Mg/m^3 in the somewhat soft and porous Btk horizon.

There were a total of four attempts at sensor installation (one on the dry site and three on the wet site), the first two of which were unsuccessful but proved informative in refining the installation procedure and redesigning the WOAT segment body for additional strength. Ultimately, two WOAT stacks comprised of four 20-cm segments each were installed that provided data in the form of TDR waveforms and initial and long-time waveform voltages, which were acquired on a near daily basis. At the time of this experiment, an automated datalogger was still in development, necessitating manual data collection.

Waveforms of 2048 points at 10 ps time increments for all functioning probes were acquired using software provided by Acclima on a laptop. Later, the waveforms were analyzed using an implementation of TACQ (Evett, 2000a,b) in MATLAB (The Mathworks, Natick, Mass.) to determine travel times.

Concurrently, independent water content data were collected with twice-weekly neutron probe (NP) observations at 12 depths 20 cm apart beginning at 10 cm in each access tube. NP soil water content was taken as the average of readings in the three access tubes on the wet side of the test site, which were 1.42, 3.99 and 6.93 m from the first WOAT stack installation site, and 4.06, 1.52 and 2.39 m from the second WOAT stack installation site. A depth control stand (Evett et al., 2003) was used in both NP calibration and field readings to ensure accuracy of probe depth and reliably accurate readings at the shallow 10-cm depth. The NP was previously field calibrated to 0.01 m^3/m^3 accuracy using methods of Evett (2008). These readings were time- and depth-matched to the TDR readings for comparison. The field plot was flooded and allowed to dry down once on DOY 263 to evaluate sensor performance over a wider range in θ.

Results

The first installation attempt was with a fully assembled, eight segment WOAT stack (160 cm length plus cutting edge) on the dry side of the test site. A diagram of the installation is shown in figure 5. Because of the high strength and cohesion of the dry clay loam, this provided an indication of the most difficult installation conditions in terms of soil penetration resistance. Installation went fairly smoothly until 60 cm of the probe stack remained above soil, at which point the auger began to bind against the cutting edge, preventing further installation. Near the end of the first installation attempt, the rear wheels of the tractor lifted off the ground as the hydraulic press pushed against the WOAT stack. Using this observation, as well as tractor test data (Nebraska Tractor Tests, 1963), we can estimate that the WOAT was under 14,700 N of force.

Communicating with the WOAT stack with a laptop revealed that only the top three sensors were active, and excavation of the partially installed WOAT stack showed that the cutting edge had been pushed away from the stack and had turned sideways, causing binding (fig. 6). Later testing of the individual WOAT segments revealed that the fourth and seventh segments had failed but the others were still functional, indicating that there was damage in the power/communications buss on the fourth segment (confirmed by testing continuity), preventing communication to the sensors below.

It appeared that as the cutting edge separated, the plastic WOAT body took the majority of the installation force rather than the steel sleeve, which was pushing only against the cutting edge that was in the softer caliche horizon at the point of failure. This led to compression of the WOAT segments and damage to the sensor circuitry, either in the circuit boards themselves or in connections between circuit boards and the buss or within the buss interconnections. Excavation revealed that the cutting edge had entered the softer caliche (Btk) horizon at the point where it was pushed ahead of the plastic WOAT stack by the steel sleeve. When the cutting edge entered the caliche, the plastic WOAT stack was held in the overlying Bt horizon with much greater cohesion, causing the plastic segments to compress while the relatively incompressible steel sleeve pushed the cutting edge through the softer caliche and away from the bottom of the stack. This revealed that the plastic WOAT segments lacked needed axial rigidity. To prevent differential movement of the WOAT stack and cutting edge under these conditions, the WOAT stack must have compressibility similar to that of the steel sleeve. Other than the circuit failures, the plastic WOAT segments did not exhibit other damage such as cracking, indicating that toughness was adequate. The second attempt was on the wet site, using the excavated and cleaned WOAT stack. This time, the cutting edge was more securely affixed using screws. Though it went in easily, the unstable pushing platform lead to the stack going in at an angle, resulting in an unacceptable gap between the sensor and the soil. Again,

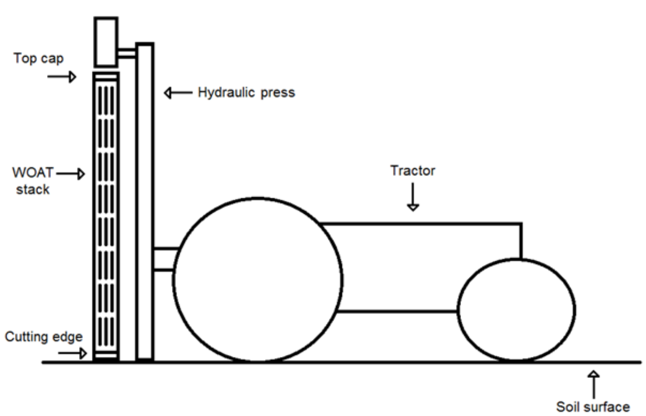

Figure 5. Diagram of first installation of fully assembled WOAT stack.

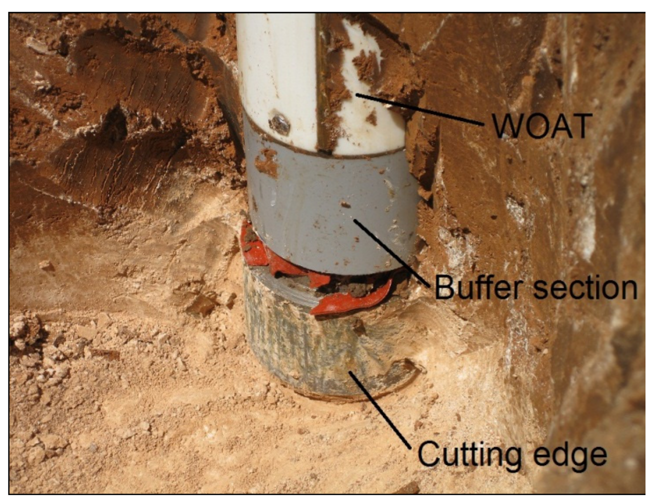

Figure 6. Separation of cutting edge from WOAT in first failed installation. The WOAT segments above the cutting edge are in the Bt soil horizon with clay content of ~50% and very high strength when dry as in this case. The cutting edge is in the more porous, lower bulk density and much softer caliche horizon with ~50% $CaCO_3$.

the sensor was excavated. For the third installation, on DOY 228, of the remaining four functional segments, we addressed the problems in the first two attempts by (1) making use of an adjustable tripod to ensure perpendicularity and (2) installing the sensor stack sequentially in order to reduce off-axis forces. If there is a stack of length L above the soil, off of perpendicular by a small angle θ, and hydraulic press force F, the moment is $FL\sin(\theta)$. Even a small moment allows bending stresses (in addition to the axial compression) to be imposed on the WOATs. By adding segments to the stack as we installed it, we reduced its length above the soil and thus its moment arm. Sequential installation of the WOAT is diagrammed in figure 7.

This installation was considered successful, though the bottom segment's waveforms indicated that the connection between the electrodes and the TDR circuit board had severed, probably due to damage incurred during the previous installations. Finally, the procedure tested on the third attempt was repeated on DOY 284 with another four segment stack once we had assembled more WOAT segments. On the final install, all sensors were functional.

Daily data collection was completed successfully, although two problems were encountered. More frequent data could not be collected due to the lack of an automated datalogger and personnel availability. Noise was encountered during the first part of the experiment but abated after around DOY 295. An example is illustrated in figure 8. It appeared to be related to wireless sensors in nearby fields using 900 MHz and 2.4 GHz communication frequencies. This noise was not severe enough to impact waveform interpretation. Additionally, there were occasional voltage spikes, which may have been due to static discharge from the power supply or poor electrical contact on a four-pin connector. The circuit board for interfacing between the WOAT stack and computer serial port was not shielded in an enclosure, which could have contributed to these problems. A direct comparison of the waveforms using the new Acclima circuits and the previous

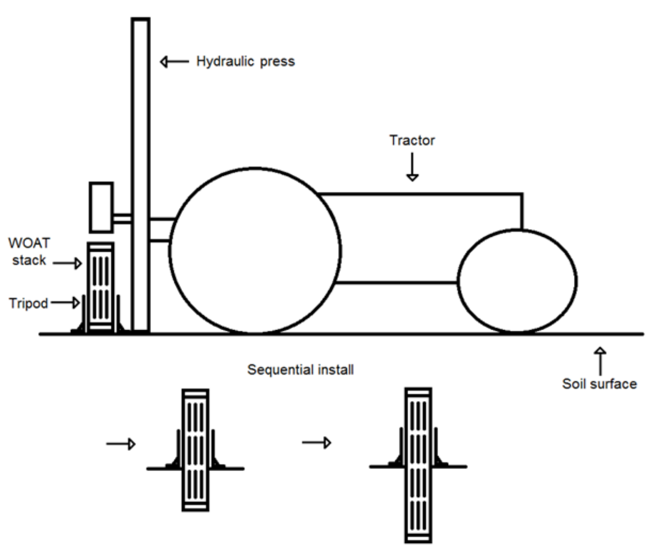

Figure 7. Sequential installation of WOAT stack. WOAT segments were added as the stack was pushed into the soil.

cabled design is given in Casanova et al. (2013). A few sensors failed over the course of the experiment. Failure occurred in one of two ways: either the sensor produced nonsense voltages instead of an interpretable waveform, or it failed to communicate entirely. The cause of this is uncertain. It could be a problem with the potting compound or moisture infiltration. The latter seems unlikely as the WOAT segment attachments were well-sealed and failures were not associated with installation forces or rain, though some of the failed sensors were those installed multiple times.

Calibration of the sensor in the laboratory gave a probe constant of 8.64 m^{-1} for BEC estimation and a volumetric soil water (VSW) response function of $t_t = 16.44\ VSW^2 - 0.53VSW + 1.40$ for the Pullman Ap layer, comparable to results obtained using similar geometry probes in Casanova (2012b). The response function is shown in figure 9. A field calibration was not attempted due to the limited number of WOAT segments installed and the failure to install in the dry site. WOAT travel times were measured from the collected waveforms and converted to water contents using the laboratory derived response function.

A time series of the average WOAT water content and NP water content for each depth, after the two successful WOAT stack installations, can be seen in figure 10. Initially, there was only the first WOAT stack, which only had functioning sensors at the top three layers, so there are no WOAT data shown for the 60- to 80-cm depth range prior to DOY 284. The top 20 cm has a lower clay content (35% to 40%) than layers below (45% to 50%), and the NP has a larger sampling radius [15 to 25 cm depending on the soil water content (Hignett and Evett, 2002)] than the TDR (1 to 2 cm). Higher clay content would lead to greater travel times at the same water content; consequently, travel times were greater for deeper layers at similar VSW.

The WOAT water content was well correlated with the NP water content in the top layer ($r^2 = 0.74$ for 0 to 20 cm), but for lower layers the limited range of water contents (i.e., 0.28 to 0.29 m^3/m^3 for 60 to 80 cm depth) makes correlation small. In the top 0 to 20 cm, the WOAT estimates of water content were smaller than those from the NP, with a bias of -0.101 m^3/m^3 and root mean square difference (RMSE) of 0.106 m^3/m^3. Differences were not unexpected since (1) sampling volumes for these two technologies differ greatly yielding different depth averaged water contents near the soil surface where there is a steep gradient in water content, and (2) the distance between NP sampling locations and WOAT sampling locations was so great that sampling volumes did not overlap and normal spatial variability in soil water content could account for the bias. Uncertainty of WOAT derived water contents was greater, possibly because of the smaller sampling volume. For 20 to 40 cm, the bias was only 0.050 m^3/m^3 and RMSE was 0.050 m^3/m^3. In the deeper layers, the WOAT estimated larger soil water content values than the NP (biases 0.125 and 0.140 m^3/m^3 for 40 to 60 cm and 60 to 80 cm, respectively, and RMSE values of 0.125 and 0.140 m^3/m^3), as the clay content was greater in these layers and the Ap calibration was not strictly applicable. The previous sensor showed similar trends with

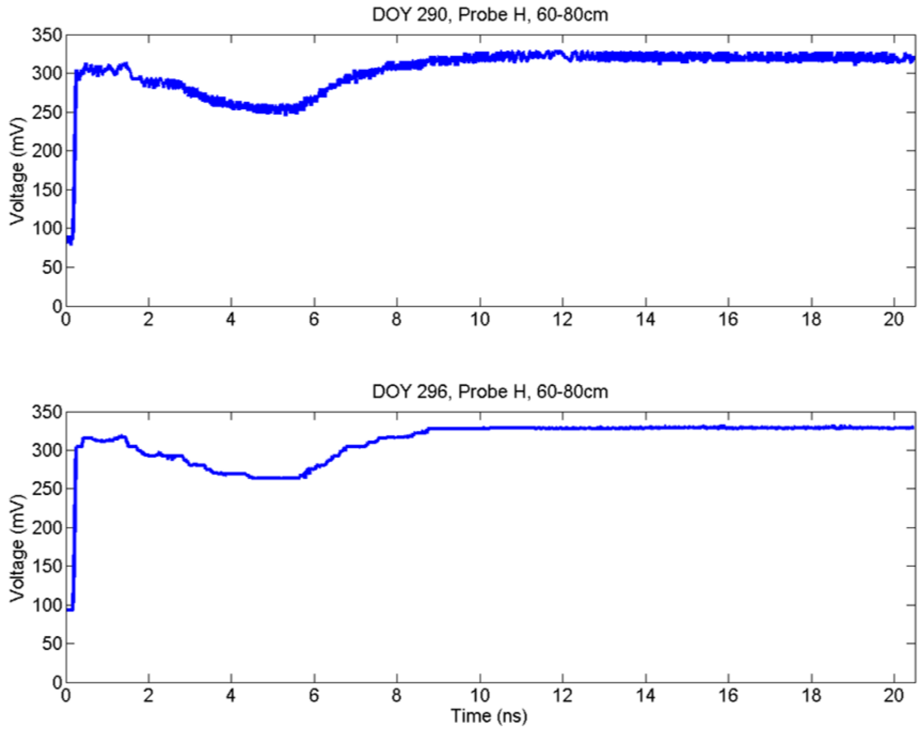

Figure 8. Examples of noise-free (DOY 296) and noisy (DOY 290) waveforms.

depth, underestimating near the surface and overestimating as depth increased (Casanova et al., 2012c). This trend is due to using a single calibration curve, despite the increase of clay content with depth. Errors were slightly higher than with the previous sensor; this could be attributed to the faster rise time of the new circuits. Faster rise time means a greater bandwidth, so the new circuits may be more sensitive to changes in clay content.

Using the laboratory calibrated probe constant and WOAT-measured initial and long term measurements, the

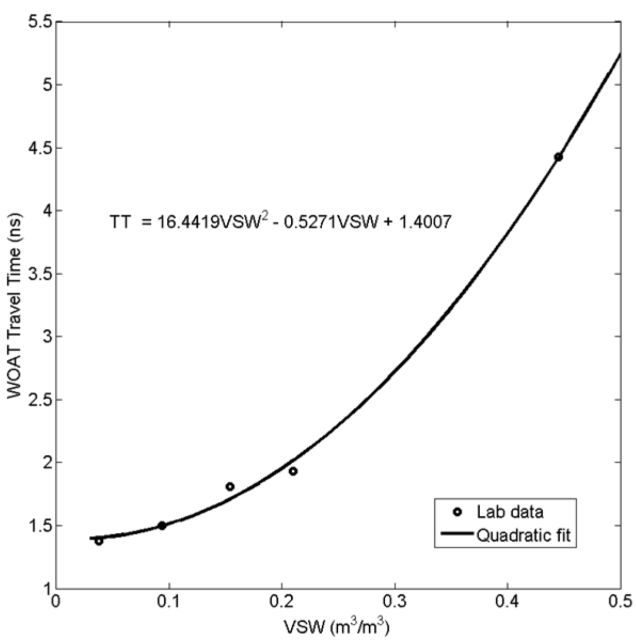

Figure 9. Lab-derived response function for the Ap (0 to 20 cm depth range) horizon.

bulk EC (BEC) was calculated for the four depths. The observed BEC data are shown in figure 11 and were within a reasonable range for this soil compared with results of Schwartz et al. (2009b) (0.1 to 0.2 S/m). Near the surface, BEC was lower (~0.05 S/m), as expected given the lower clay content in the top 20 cm.

CONCLUSIONS

In this article we presented a novel sensor for measuring a soil water content profile, a waveguide-on-access-tube (WOAT). The WOAT's segmented design and embedded TDR circuits directly coupled to the measurement electrodes allow for an easier assembly process and construction of probe stacks of arbitrary length, compared to the previous design (Casanova et al., 2012c). Field tests revealed that the sensor must be designed to be mechanically stronger for installation in the most difficult soils (soils with high penetration resistance). Successfully installed sensors enabled collection of quality TDR waveforms and long-time voltages, which when properly calibrated, can be converted to soil water contents and bulk electrical conductivity. Lab calibration of the sensor and comparison of field data with neutron probe measurements were generally favorable, though the difference in soil properties with depth, the difference in sampling volumes and spatial separation of sampling sites, and the limited range of observed water contents led to some discrepancies. Overall, the WOAT design was successful, but mechanical strength and stiffness must be increased for installation in the most difficult soils, and a more generalized electromagnetic mixing model must be established to reduce the need for site-specific calibrations.

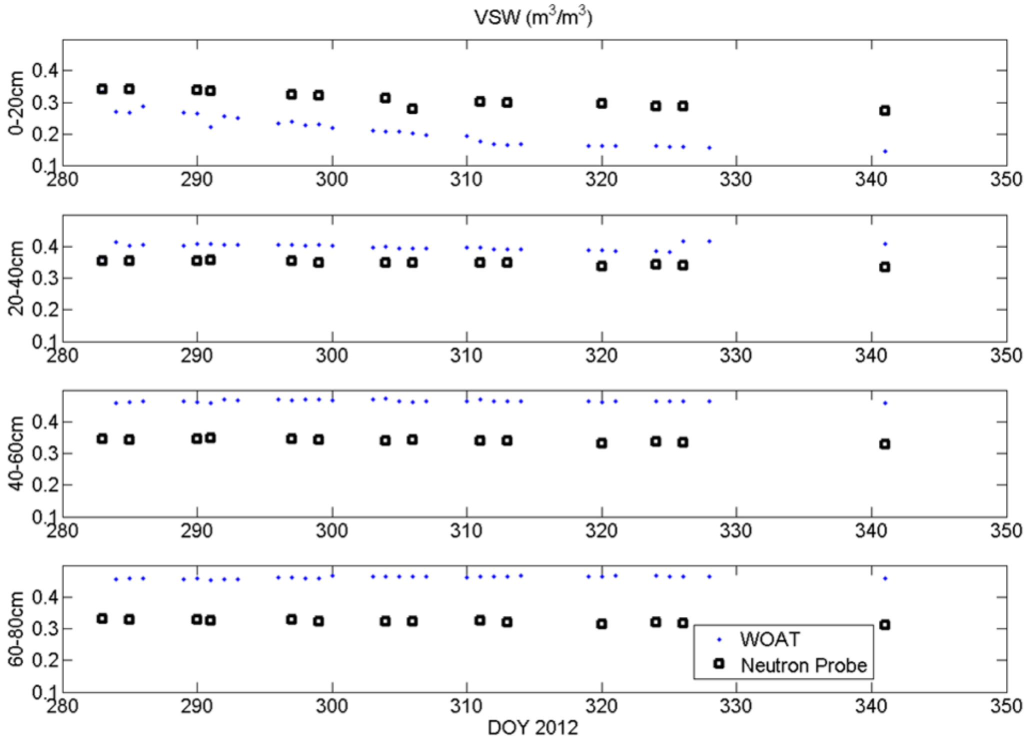

Figure 10. Time series of volumetric water contents (VSW) from neutron probe (NP) and WOAT sensors, by depth.

ACKNOWLEDGEMENTS

We gratefully acknowledge the technical assistance of Mr. Brice Ruthardt for help in probe construction. This research was supported by the Ogallala Aquifer Program, a consortium between USDA-Agricultural Research Service, Kansas State University, Texas A&M AgriLife Research, Texas A&M AgriLife Extension Service, Texas Tech University, and West Texas A&M University.

REFERENCES

Anderson, S. K. 2009. Two-conductor moisture activated switch. U.S. Patent No. 7,562,832.

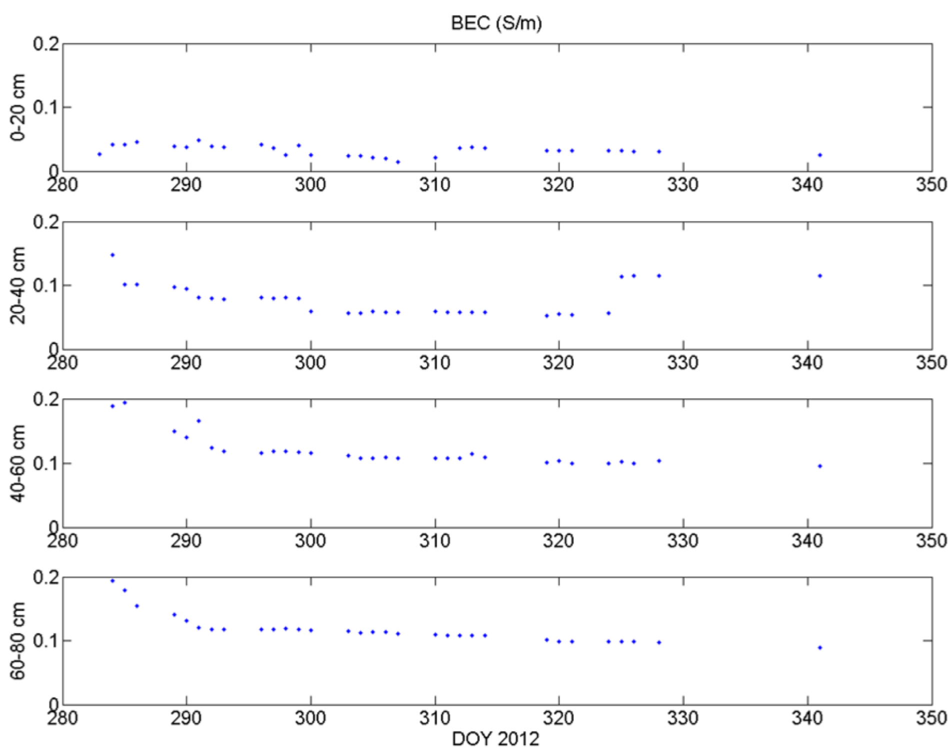

Figure 11. Time series of bulk electrical conductivity (BEC) values from WOAT TDR sensors, by depth.

Casanova, J. J., Evett, S. R. & Schwartz, R. C. 2012a. Design of access-tube TDR sensor for soil water content: Theory. *IEEE Sensors J. 12*(6): 1979-1986.

Casanova, J. J., Evett, S. R., & Schwartz, R. C. 2012b. Design of access-tube TDR sensor for soil water content: Testing. *IEEE Sensors J. 12*(6): 2064-2070.

Casanova, J. J., Evett, S. R., & Schwartz, R. C. 2012c. Design and field tests of an access-tube soil water sensor. *Applied Eng. in Agric. 28*(4): 603-610.

Casanova, J. J., Schwartz, R. C., Evett, S. R., & Anderson, S. K. 2013. Directly coupled vs. conventional time domain reflectometry in soils. *Applied Eng. in Agric. 29*(5): 771-777.

Evett, S. R. 1998. Coaxial multiplexer for time domain reflectometry measurement of soil water content and bulk electrical conductivity. *Trans. ASAE 41*(2): 361-369.

Evett, S. 2000a. The TACQ computer program for automatic time domain reflectometry measurements: I. Design and operating characteristics. *Trans. ASAE 43*(6): 1939-1946.

Evett, S. 2000b. The TACQ computer program for automatic time domain reflectometry measurements: II. Waveform Interpretation Methods. *Trans. ASAE 43*(6): 1947-1956.

Evett, S. R., Tolk, J. A., & Howell, T. A. 2003. A depth control stand for improved accuracy with the neutron probe. *Vadose Zone J. 2*(4): 642-649.

Evett, S., Heng, L., Moutonnet, P., & Nguyen, M. 2008. Field estimation of soil water content: A practical guide to methods, instrumentation and sensor technology. IAEA-TCS-30.International Atomic Energy Agency, Vienna, Austria.

Evett, S. R., Schwartz, R. C., Tolk, J. A., & T. A. Howell. 2009. Soil profile water content determination: Spatiotemporal variability of electromagnetic and neutron probe sensors in access tubes. *Vadose Zone J.* 8(4): 926-941.

Evett, S. R., Schwartz, R. C., Casanova, J. J., & Heng, L. K. 2012. Soil water sensing for water balance, ET and WUE. *Agric. Water Manage. 104*: 1-9.

Hignett, C., & Evett, S. R.. 2002. Neutron thermalization. Section 3.1.3.10. In *Methods of Soil Analysis. Part 4 - Physical Methods*, 501-521. J. H. Dane and G. C. Topp, eds. Madison, Wisconsin: Soil Science Society of America.

Lin, C., Chung, C., Huisman, J. & Tang, S. 2008. Clarification and calibration of reflection coefficient for electrical conductivity measurement by time domain reflectometry. *Soil Sci. Soc. Am. J. 72*(4): 1033-1040.

Merriam, J. 1966. A management control concept for determining the economical depth and frequency of irrigation. *Trans. ASAE 9*(4): 492-498.

Nebraska Tractor Tests. 1963. Test 848: John Deere 3020 Diesel. Paper 399.

Redeye. 2008. ABS Material Specifications. http://redeyeondemand.com/ downloads/MSpec_ABS.pdf. Accessed 13 March 2013.

Schwartz, R. C., Evett, S. R., & Bell, J. M. 2009a. Complex permittivity model for time domain reflectometry soil water content sensing: I. Theory. *Soil Sci. Soc. Am. J. 73*(3): 886-897.

Schwartz, R. C., Evett, S. R., & Bell, J. M. 2009b. Complex permittivity model for time domain reflectometry soil water content sensing: II. Calibration. *Soil Sci. Soc. Am. J. 73*(3): 898-909.

Topp, G., Davis, J. & Annan, A. 1980. Electromagnetic determination of soil water content: Measurements in coaxial transmission lines. *Water Resources Res. 16*(3): 574-582.